Annals of Biomedical Research
An open access journal
eSciRes
ABR-1-112
Research Article

Force-field Dependency of Leu-rich Helical Peptides Dimerization Energy in Lipid Bilayers. I. United-atom Simulations Show Discrepancy from Experiments and All-atom Simulations

Nishizawa M and Nishizawa K*
Teikyo University School of Medical Technology, Itabashi, Japan

Abstract

United-atom (UA) description of aliphatic carbon-hydrogen atoms with single particles have been used in simulation analyses of protein/lipid systems. However, UA force fields (FFs) simulations have shown inaccuracy in transmembrane (TM) helical peptides dimerization dynamics within lipid membranes. For example, the self-dimerized state of a TM helical peptide $(AALALAA)_3$ in a phospholipid bilayer is unrealistically unstable in simulations under two FFs, namely, the OPLS-all atom (AA) protein/Berger UA lipids and GROMOS 53A6 (Gr^{53a6}) FFs, whereas AA Charmm36 (Ch^{36AA}) FF showed a dimerization energy comparable with the experiment. Here we show that the dimer stability of a Lys-flanked poly-Leu peptide (KL22) exhibits no or little dimerization propensity with Gr^{53a6}, but shows dimerization propensity of the free energy of −7.5 kJ/mol with Ch^{36AA} comparable to the experiment (−8.3 kJ/mol). A peptide comprised solely of Leu (L21) showed similar FF-dependency. Although the dimer stability was fairly similar between Ch^{36AA} and Gr^{53a6} for both poly-Ile and poly-Val helices, a Ch^{36AA}>Gr^{53a6} stability difference was also seen for poly-Ala helices. While the UA parameters have normally been adjusted guided by the experiments with simple systems using the amino acid side chain analogues, the findings presented here highlight limited transferability of UA parameters to the settings of peptides/lipid membranes.

Introduction

Characterization of dynamics of proteins in biomembranes allows many biomedical problems to be answered at the molecular level. Interactions between transmembrane (TM) peptide domains have been implicated in a number of phenomena ranging from folding to functions of membrane proteins and to coordinated function of membrane protein complexes [1,2]. Such interactions are often dynamic, and switching between distinct interaction modes has been implicated in several receptor tyrosine kinases involving EGFR [3-5]. Fine-tuning of the TM-TM interaction energetics is considered important in many cases, as evidenced by a number of diseases caused by mutations within TM domains [3,6,7]. For many of such TM segments, dynamic interactions appear important, and TM interactions are likely mainly mediated by van der Waals interactions, rather than strongly polar or charged residues [3]. More recently, for several hormone and cytokine receptors, not only the presence of inactive dimers but also the subsequent ligand-induced structural changes important for activation have been shown, implying that relatively loose and dynamic associations between TM domains can be considered a basis for many cellular signal transductions [7,8].

Molecular dynamics (MD) simulation is a useful tool for analyzing lipid-peptide interaction. Recent studies of energetics of dimerization of helical peptides are mainly addressed through CG simulations [e.g,. 9,10]. Likely due to computational burden, direct measurements of the free energy for association (dimerization, binding) of TM helical peptides in atomistic models of lipid membranes have been limited. Henin et al. calculated the dimerization free energy of the TM helix of GpA in a dodecane slab [11], but to our knowledge the dimerization free energy quantification based on an explicit atomistic representation of a phospholipid membrane has been elusive.

Although atomistic force-fields (FFs) are generally considered more accurate than CG FF in many settings, our recent analyses unexpectedly showed that UA simulations sometimes show unrealistic results [12,13]. For instance, under the OPLS-AA (optimized potentials for liquid simulations-all atom) [14]/Berger (or OB) FF [15], both a WL15 $(GWW(L)_9WWA)$/DLPC bilayer and a WALP15 $(GWW(LA)_4LWWA)$/DLPC bilayer systems showed only repulsive mean forces and therefore no propensity for TM self-dimerization throughout the tested range of distance, whereas CG-based measurement showed clear dimerization propensity [16]. When we measured the dimerization energy of $(AALALAA)_3$ under two united-atom (UA) force fields (FFs), i.e., OB and GROMOS 53A6 (Gr^{53a6}) [12] in a setting similar to the experiments [17], both of the latter UA FFs exhibited poor dimerization propensities, the self-association free energy with OB being −4.4 kJ/mol, and that with Gr^{53A6} being −5.2 kJ/mol, respectively, which were significantly smaller than the experimental value (−12.7 kJ/mol). Similar analysis with all-atom (AA) Charmm36 (Ch^{36AA}) yielded −9.9

kJ/mol, which was more comparable to the experimental value. These suggested superior accuracy of Ch^{36AA} at least for this setting. However, AA simulations demand 3 to 5-fold computation compared to UA GROMOS FF [12,18], depending on the proportions of the water/lipids/proteins, rationalizing the efforts to improve UA FFs aiming for reduction of computational burden.

TM-TM association energetics can be considered to be mainly governed by three components; the direct (specific) peptide-peptide interaction energy $V_{pept-pept}$, the specific $V_{lipid-pept}$ interaction energy (i.e., the energy for solvation of TM peptides by lipids) and the specific lipid-lipid interaction energy $V_{lipid-lipid}$ [9]. Too (energetically) favorable solvation of amino acid residues by lipids increases the cost for desolvation, disfavoring TM-dimerization. For the evaluation of the FF accuracy in the analyses of TM interactions, the energetics amino acid side chain (SC)-SC interactions in apolar solvents have been used as a reference. Marrink and coworkers compared MARTINI CG, GROMOS and OPLS-AA FFs in dimerization energy of SCAs in polar and nonpolar solvents [19]. Feig and coworker used Ch^{36AA} (for lipids) and Charmm General FF for side chain analogues (SCAs) to measure the energetics of dimerization for several SCAs at various insertion depths into lipid bilayer [20]. Of note, both studies showed remarkable differences among the FFs, suggesting a worrisome challenge in parameterization in protein/lipid simulations [19]. Further, it still remains unclear how such differences in the SCAs analyses are linked to the inaccurate TM dimerization energetics. It is of importance to understand the relationship among solvation and dimerization of SCAs in apolar solvents and their relationship to helix-helix interaction. In particular, our interest is the issue whether the aforementioned inaccuracy in the TM dimerization under UA FFs could be attributed to SCA solvation or dimerization energy.

In this study, based on the potential of mean force (PMF) computations totaling 315μs (105μs AA and 210μs UA simulations), we examine TM dimerization propensity for peptides other than $(AALALAA)_3$. For the Lys-flanked poly-Leu peptides used in Mall et al. [21], Ch^{36AA} showed dimerization propensity comparable to the experiment whereas Gr^{53a6} showed little such propensity. Self-dimerization of a poly-Ile as well as a poly-Val helix showed a relatively better agreement between the two FFs.

In our companion paper [22], the energetics of solvation and self-association of several SCAs in apolar solvents are computed. These results lead us to discuss the potential benefits of our simple reparameterization method that downscales only the Lennard-Jones (LJ) terms between protein and lipid, guided by the TM helix dimerization energy based on AA simulations as the reference.

Methods

Simulation systems

Molecular dynamics simulations were performed using the Gromacs package version 4.5.4. OPLS-all atom (AA) and Berger force fields and their combination were used as previously described [23]. Gr^{53a6} protein FF and the SPC water model were used as implemented in the Gromacs version in combination with the GROMOS $53A6_L$ lipid FF by Poger et al. [24] after downloading from Lipidbook [25]. Of note, the GROMOS $53A6_L$ was derived based on the standard Gr^{53a6} parameters [26] and using the charges for lipid of Chiu et al. with some modifications into van der Waals interactions between the methyl groups of the choline group and the phosphate oxygen atoms of the lipid head groups [27,28]. As Ch^{36AA}, the parameter file charm36-jun2015.ff [29] was used for peptides and lipids provided by Dr MacKerell (http://mackerell.umaryland.edu/charmm_ff.shtml) [30]. From the DOPC parameters thereof, we adopted parameters for octane and dibutyrylphosphatidylcholine (diC_4PC). For Ch^{36UA}, the topology parameters provided by Lee et al. [31] were used. The latter UA FF uses the lipid parameters derived by modifications of OPLS-UA [32] in combination the Ch^{36AA} parameters for proteins. These parameters are tabulated in the Appendix Table A1.

We used the model peptides listed below:

$(AALALAA)_3$: AALALAAAALALAAAALALAA

$KL22_W$: $KKG(L)_{10}W(L)_{12}KKA$

$KL22_Y$: $KKG(L)_{10}Y\ (L)_{12}KKA$

Ki23: $KKGI_{23}KKA$

Leu21 (or L21): LLLLLLLLLLLLLLLLLLLL

Ile21: IIIIIIIIIIIIIIIIIII

Val21 (or V21): VVVVVVVVVVVVVVVVVVVV

Ala21 (or A21): AAAAAAAAAAAAAAAAAAAA

$KL22_w$ and $KL22_Y$ are the Lys-flanked Leu-rich peptides that were referred to as L_{22} and Q_{22} in Mall et al. [21], respectively, although in the latter peptide, the dibromotyrosine was replaced with Tyr in the present study. For their Lys side chains, the protonated state (+1 charge) was used. In Mall et al. [21], the orientation between the two peptides (i.e., parallel *vs.* anti-parallel) was not discriminated. Parallel *vs.* anti-parallel comparison of KL22 dimerization based on the Ch^{36UA} system showed a small difference (~0.6 kJ/mol) (#4 and #5 of Table 1), and this does not influence the conclusion of this study. The N- and C-termini were capped with acetyl group and $-NH_2$ group, respectively. The initial structures of helical $(AALALAA)_3$ peptides and the equilibrated atomistic DOPC and octane/diC_4PC models were taken from our recent simulations [12] and the structures of the other peptides were derived by modification of those of the $(AALALAA)_3$.

sim ID	simulation title, (orientation: ap, anti-parallel; p, parallel)	distance of PMF minimum (Å)	ΔG^{dim} ±S.E. (kJ/mol)	system (range for umbrella window)[1)]	experimental ΔG^{dim} (kJ/mol)[2)]
#1	Gr-KL22-dopc (ap)	repulsive	-1.55 ± 1.00	doS (0.7-1.6)	-8.3
#2	Gr-KL22-oc/diC$_4$PC (ap)	repulsive	-0.32 ± 0.22	ochS (0.7-1.6), ochL (1.6-2.0)	n.d
#3	Ch^{UA}-KL22-dopc (ap)	11.2	-3.31 ± 0.28	doS (0.9-1.6)	-8.3
#4	Ch^{UA}-KL22- oc/diC$_4$PC (ap)	repulsive	-0.93 ± 0.14	ochS (0.9-1.6), ochL (1.6-2.0)	n.d
#5	Ch^{UA}-KL22- oc/diC$_4$PC (p)	13.5	-1.53 ± 0.41	ochS (0.9-1.6)	n.d
#6	Ch^{AA}-KL22-dopc (ap)	10.0, 11.6 (two troughs)	-7.46 ± 2.04	doS (0.9-1.6)	-8.3
#7	Ch^{AA}-KL22- oc/diC$_4$PC (ap)	11.5	-3.77 ± 0.57	ochS (0.9-1.6)	n.d
#8	Gr-L21-dopc (ap)	repulsive	-0.24 ± 0.80	doS (0.9-1.6), doL (1.6-2.0)	n.d
#9	Ch^{AA}-L21-dopc (ap)	10	-6.12 ± 2.00	doS (0.9-1.6)	n.d
#10	Gr-L21- oc/diC$_4$PC (ap)	repulsive	-0.34 ± 0.36	ochS (0.8-1.6), ochL (1.6-2.0)	n.d
#11	Ch^{AA}-L21- oc/diC$_4$PC (ap)	10.5	-2.40 ± 0.58	ochS (0.8-1.6)	n.d
#12	Gr-Ki23- oc/diC$_4$PC (ap)	repulsive	-0.46 ± 0.29	ochS (0.7-1.6), ochL (1.6-2.0)	n.d
#13	Ch^{AA}-Ki23- oc/diC$_4$PC (ap)	12.5	-1.55 ± 0.17	ochS (0.8-1.6)	n.d
#14	Gr-Ile21-oc/diC$_4$PC (ap)	12.4	-1.24 ± 0.16	ochS (1.0-1.6), ochL (1.6-2.0)	n.d
#15	Ch^{AA}-Ile21- oc/diC$_4$PC (ap)	12.1	-1.14 ± 0.13	ochS (1.0-1.6)	n.d
#16	Gr-V21-oc/diC$_4$PC (ap)	11	-1.14 ± 0.31	ochS (0.9-1.6), ochL (1.6-2.0)	n.d
#17	Ch^{AA}-V21- oc/diC$_4$PC (ap)	11.5	-1.20 ± 0.09	ochS (0.9-1.6)	n.d
#18	Gr-A21-oc/diC$_4$PC (ap)	7.8	-1.95 ± 0.25	ochS (0.7-1.6), ochL (1.6-2.0)	n.d
#19	Ch^{AA}-A21- oc/diC$_4$PC (ap)	8.9	-3.86 ± 0.54	ochS (0.7-1.5)	n.d

In the simulation title, Gr, Ch^{AA} and Ch^{UA} stand for Gr^{53a6}, Ch^{36AA} and Ch^{36UA}, respectively.

[1)] For example, "doS (0.7-1.6), doL (1.6-2.0)" indicates that windows of r = 0.7, 0.8.,...1.6 nm were used for the near range (with the box doS) and the 1.6, 1.7, .. 2.0 nm windows were used for the far range (with the box doL). The system components were as follows. ochS, 136 octane/56 diC$_4$/2047 water; ochL, 209 octane/86 diC$_4$PC/2640 water; doS, 56 DOPC/2047 water; doL, 86 DOPC/2640 water. Simulation time was 4×400ns×15 (ochS and doS) and 4×400ns×7 (ochL and doL)[2)] -8.3 kJ/mol is based on [ref. 21]. n.d. stands for 'not determined to our knowledge'.

Table 1: Helix dimerization PMF analyses performed in this study.

For all simulations, bond lengths of peptides were constrained using the LINCS algorithm [33], whereas the bonds and angles of water were constrained using the SETTLE algorithm [34]. The LJ interactions were smoothly cut off using a switch function from 0.8 to 1.3 nm. Long-range electrostatic interactions were treated using the particle-mesh Ewald (PME) method [35] with a real cutoff of 1.49 nm and with a grid-spacing of 0.15 nm. The time step of 3.3 fs was used. The temperature was kept at 323 K and pressure was controlled at 1 bar with the isotropic coupling for octane/diC$_4$PC and cyclohexane systems and the semi-isotropic coupling for the DOPC systems, respectively.

PMF analysis of TM dimerization

The potential mean force (PMF) analysis of free energy of peptide dimerization was performed as we have described [12,13]. To prepare the initial structures of dimerization PMF analyses, the helices were inserted to membrane(s) and six lipid molecules including the overlapping ones were moved manually and subjected to the equilibration runs. The pull-code program of Gromacs was used to impose a harmonic potential (umbrella potential) with a coefficient of 3000 kJ/mol/nm^2 on the distance r between the centers of mass (COMs) of the two peptides. As in our recent reports, two distinct system sizes were used for the near and far ranges (Table 1) in order to save the computation time. The windows for the umbrella sampling were set as shown in Table 1 and with a 0.1 nm interval. Of note, for the Ch^{36AA} and some Ch^{36UA} and Gr^{53a6} analyses, only the small membrane and accordingly only the narrower range (for example, 0.9−1.6 nm) was used (Table 1).

The force outputs (pullf.xvg of Gromacs) were merged as if they were derived from the same set of umbrella sampling upon the weighted histogram analysis method WHAM analysis [36], the latter yielding the PMF profile, $G^{PMF}(r)$, where r represents the interhelical separation. The dimerization free energy ΔG^{dim} for helical peptides was calculated as $\Delta G^{dim} = -RT \ln K_a$, where K_a is the ratio of the time length during which the two peptides are in dimer to that during which they are in monomers and was estimated as $K_a = [\int_{0.8}^{Rc} \pi r^* g(r)\, dr]/P_m$. Here, R_c is the cutoff that defines the dimerized state, g(r) is the two-dimensional radial distribution function (rdf) profile obtained by compensating the

Boltzmann factor $\exp(-\beta G^{PMF}(r))$ with respect to the r-dependent increase in available phase space, and the normalization factor P_m is given as $P_m = [v/\pi*(R_{max}^2 - R_c^2)] * [\int_{Rc}^{Rmax} \pi r*g(r)\, dr]$, where v is the bilayer area available to a peptide monomer at the standard concentration. Note that P_m is equivalent to normalized v, that is, v weighted by the time length during which the two peptides are in monomers estimated by the integration. In the current study, R_c = 1.6 nm and v=1.66 nm^2 were used (as in [13]). Of note, for the Ch^{36AA} sets, the umbrella sampling was not performed for the range of r>1.6 nm, and, hence, K_a was derived assuming the flatness of the rdf profile g(r) for r>1.6 nm. Thus, the Ch^{36AA} data should have additional inaccuracy due to this treatment.

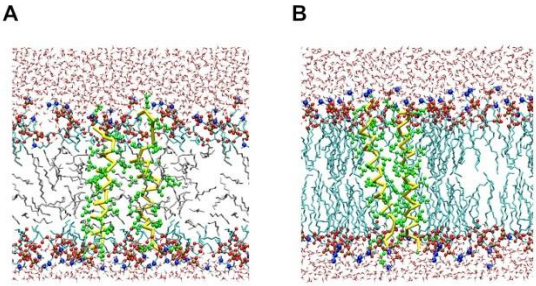

Figure 1: Representative snapshots of the dimerization PMF simulations. As examples, the systems for the poly-Leu peptides (KL22$_W$ and KL22$_Y$) are shown. (A) The octane/diC$_4$PC system (#2 of Table 1). In this example the interhelical distance r was held at 1.6 nm. Representation scheme: silver licorice, octane; spheres of middle size (ochre, red, and blue), diC$_4$PC (phosphorus, oxygen, and nitrogen atoms, respectively); yellow trace, peptide backbone; green spheres, Leu side chains (SCs); thin licorice (silver and red), water atoms. Only lipid molecules located within a 2.0-nm-thick slice are shown. (B) The dioleoylphosphatidylcholine (DOPC) bilayer system (#1 of Table 1) with r was constrained at 1.1 nm. Representation scheme is similar to (A), but cyan licorice represents hydrocarbon chains of DOPC.

Results

Poly-Leu helix self-associates in lipid membranes under Charmm36 but not under GROMOS 53A6 parameters

The TM dimerization PMF analysis performed in this study are listed in Table 1 (Sim ID: #1-16). The simulation sets have three-part names (e.g., Gr-(AALALAA)$_3$-octane/diC$_4$PC); the first part represents the FF used, the second represents the peptide and the third represents the lipid membrane (or solvent). The settings and simulation time periods are similar to our previous analyses [12,13]. Graphical presentation of some simulations is given in Figure 1.

Strikingly, for the Lys-flanked poly-Leu peptides (i.e, KL22$_W$ and KL22$_Y$), Gr^{53a6} systems exhibited repulsive forces (no attractive force) in DOPC throughout the interhelical distances tested, as shown by the PMF profiles (sim #1 of Table 1 and Figure 2A). Of note, even a repulsive PMF curve can yield a negative ΔG^{dim} value likely due to the definition of the 'dimeric state'. We also performed a similar set of simulations using the octane slab covered by PC with short-alkyl chains (octane/diC$_4$PC), which helps to improve statistical convergence relative to the DOPC bilayer. The dimer was remarkably unstable in the octane/diC$_4$PC under Gr^{53a6} as well (#2). In contrast, Ch^{36AA} exhibited a dimerization energy of −7.5 kJ/mol (#6, DOPC) and −3.8 kJ/mol (#7, octane/diC$_4$PC), the former being comparable with the experimental energy (−8.3 kJ/mol) (Figure 2B). We also tested Ch^{36UA}, which utilizes the Ch^{36AA} model for KL22$_W$ /KL22$_Y$ in combination with an UA model for lipids [31], but this showed poor dimerization propensity in the DOPC and in octane/diC$_4$PC membrane (#3 and #4) relative to the corresponding Ch^{36AA} simulations (#6 and #7). We mainly focused on the antiparallel-orientation, but the parallel orientation was also tested for the Ch^{36UA} system. This showed a slightly more significant binding energy for Ch^{36UA} (set #5) relative to the antiparallel settings, yet, by merging the Boltzmann factor for the parallel and anti-parallel results, we obtain the dimerization energy for Ch^{36UA} much weaker than the experiment (−8.3 kJ/mol) [21]. Overall, for the Lys-flanked poly-Leu peptides, the dimerization propensity showed differences of the order of: the experiment [21] > Ch^{36AA} > Ch^{36UA} > Gr^{53a6}. When the Leu21 that was devoid of the flanking Lys residues was examined, both the DOPC (#8 and #9) and octane/diC$_4$PC (#10 and #11) sets showed a difference of Ch^{36AA} > Gr^{53a6} in the propensity similar to the above. These findings call for a careful interpretation of simulation results with Leu-rich TM helical peptides embedded with lipid membranes under UA FFs (Figure 2).

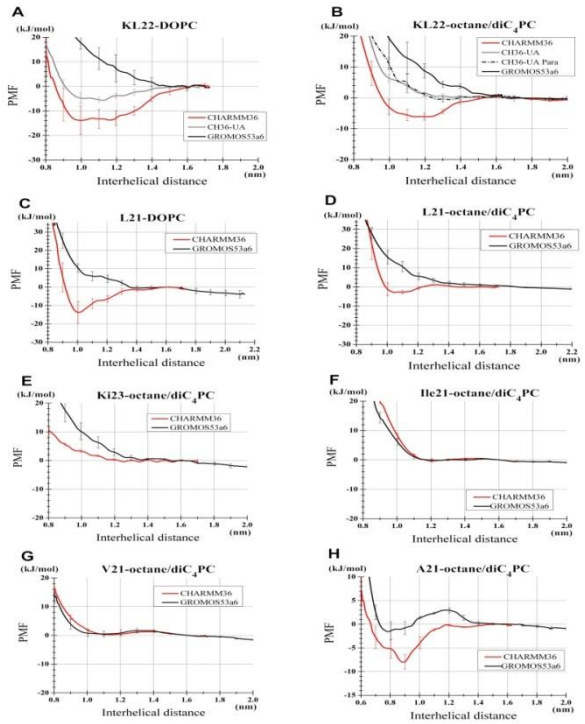

Figure 2: Comparison among the FFs in the dimerization PMF profiles. (A) The KL22/DOPC systems (#1, #3 and #6 of Table 1). Error bars represent SEs from four independent umbrella analysis sets. The values relative to

the average of the values at r=1.6 nm are plotted. Of note, this umbrella sampling was done for the range ≤ 1.6 nm, but the WHAM analysis yielded the profile up to 1.7 nm (B) The KL22/octane/diC$_4$PC systems (#2, #4 and #7). The result for the peptides placed in the parallel orientation is also shown ('Ch36UA-Para', #5 of Table 1). Presentation scheme is similar to (A). (C) The L21/DOPC systems (#8 and #9). (D) L21/octane/diC$_4$PC systems (#10 and #11). (E) Ki23/octane/diC$_4$PC systems (#12 and #13). (F) Ile21/octane/diC$_4$PC systems (#14 and #15). (G) V21/octane/diC$_4$PC systems (#16 and #17). (H) A21/octane/diC$_4$PC systems (#18 and #19).

Ile-, Val- and Ala-rich peptide self-association analyses show differing levels of GROMOS-Charmm discrepancy

When the Lys-flanked poly-Ile peptide (Ki23) was used, the dimerization propensity as well as PMF profile was largely similar between Gr^{53a6} (#12) and Ch^{36AA} (#13) for the octane/diC$_4$PC (Figure 2E). The poly-Ile peptide Ile21 that was with no flanking Lys residues also showed a negligible between-FF difference in the octane/diC$_4$PC (#14 and #15, Figure 2F). However, this has to be carefully interpreted as we recently found that, in the *DOPC* bilayer, the dimerization energy for Ile21 (that lacked the flanking Lys residues) was different between Gr^{53a6} (0.23 kJ/mol) and Ch^{36AA} (−1.75 kJ/mol) [13]. Therefore, the FF-dependency could become problematic also for Ile-rich peptides in some settings, although it may not be as severe as in the case with the Leu-rich peptides.

For the poly-Val (V21) peptide, Ch^{36AA} and Gr^{53a6} also showed no appreciable difference in the octane/diC$_4$PC (#16 and #17, Figure 2G). However, for the poly-Ala helix, Ch^{36AA} led to stable dimerization compared to Gr^{53a6} (#18 and #19 and Figure 2H). Of note, we previously showed that, both of the UA FFs (i.e., OB and Gr^{53a6}) underestimate the stability of dimer of the (AALALAA)$_3$ helical peptide in the DOPC bilayer as well as in the octane/diC$_4$PC [12], whereas the simulations with Ch^{36AA} yielded dimerization propensity comparable to the experiments by Yano et al. (Table 2).

Of note, the comparison among the simulations performed under the same FF and with the same membrane (for example, # 8 and #21, #11 and #26) demonstrates that the presence of Ala residues stabilizes the dimeric state, which can be explained by the small size of Ala side chain that allows close association of the two helices (i.e., the small values of the distance that showed the PMF minimum in Table 2), which leads to a larger electrostatic energy.

Conclusion

In this and previous studies, we showed that the UA models, GROMOS (Gr^{53A6}) and OB, tend to show significantly weak propensity of helix peptides dimerization within explicit phospholipid membranes for various peptides, and especially, for Leu-rich peptides, compared to the AA model and the experiments. The discrepancy of Gr^{53A6} from Charmm36 (Ch^{36AA}) in the TM self-dimerization energy for the poly-Ile and poly-Val peptides was not excessive, but significant for the poly-Ala peptide. In a companion paper, we show data which are indicative of limited transferability of UA FFs in the settings in which the peptide-peptide interactions are studied in hydrated phospholipid membranes.

The limitations of this study should be considered. While our use of the simple model peptides and independently prepared initial structures should have improved the sampling by the 400ns simulation per umbrella sampling window, further computation is necessary for more rigorous comparison among the FFs. More importantly, the computational burden prohibited us from computing the range > 2.0 nm in this study. So our study should be regarded as a near-range behavior analysis; to our knowledge, the interhelical mean forces for the model peptides placed with a >2 nm interval have not been measured in atomistic simulations like ours, and this issue need to be addressed in future analyses. As another limitation, we mainly used octane/diC$_4$PC. The data derived with the latter system were not the same as those from the corresponding DOPC system. Intriguingly, except for the cases with (AALALAA)$_3$ peptides (Table 2), the use of the octane/diC$_4$PC slab tended to destabilize the dimeric state compared to the DOPC bilayer.

sim ID	simulation title[1)]	distance of PMF minimum (Å)	ΔG^{dim} ±S.E. (kJ/mol)	experimental ΔG^{dim} (kJ/mol)[2)] [ref.17]	reference
#20	Gr-(AALALAA)$_3$-oc/diC$_4$PC	9.1	-2.03 ± 0.71	n.d.	this study[3)]
#21	Gr-(AALALAA)$_3$-dopc	7.9	-5.2 ± 1.0	-12.7	[12]
#22	Ch^{UA} -(AALALAA)$_3$-oc/diC$_4$PC	7.8	-3.45 ± 1.44	n.d.	this study[3)]
#23	OB-(AALALAA)$_3$-dopc	8.1	-4.4 ± 1.4	-12.7	[12]
#24	OB-(AALALAA)$_3$-oc/diC$_4$PC	8.6	-5.5 ± 1.5	n.d.	[12]
#25	Ch^{AA}-(AALALAA)$_3$-dopc	7.7	-9.9 ± 1.3	-12.7	[12]
#26	Ch^{AA}-(AALALAA)$_3$-oc/diC$_4$PC	7.8	-12.5 ± 1.1	n.d.	[12]

[1)] In the simulation title, OB, Gr, Ch^{AA} and Ch^{UA} stand for OPLS-AA/Berger. Gr^{53a6}, Ch^{36AA} and Ch^{36UA}, respectively. All simulations shown in this table used the peptides placed in the anti-parallel configuration. [2)] n.d. stands for 'not determined to our knowledge'. [3)] For #20 and #22, the umbrella window range of 0.7–1.6 nm was computed with the system ochS (136 octane/56 diC$_4$/2047 water).

Table 2: (AALALAA)$_3$ dimerization PMF analyses including our recent studies.

From our recent analysis with raft-like bilayers and the DOPC bilayer [13], it is possible that head group can coordinate the monomeric peptides well in the octane/diC_4PC system, stabilizing the monomeric state. However, this does not hold for the $(AALALAA)_3$ sets (Table 2). Clearly, this argument requires further analyses.

We would like to comment on the amino acid composition of helical TM domains of membrane proteins. In the analysis by Liu et al. that used the amino acid sequences of TM helices from 168 families [37], each with 20 or more members showed that TM helices are comprised of Leu (16%), Ile (10%), Ala (9%), Phe (8%), Gly (8%), Val (8%), Ser (7%), Thr (7%), and other amino acids each accounting for <5% [37] (Table 3).

Intriguingly, the collection by Moore et al. [3] of disease-related single-pass TMs relevant for cellular signaling showed a composition biased toward V, L, and I; for the 13 sequences sampled from the Moore et al.'s list by removing related entries, L, I, and V accounted for 51% in sum, which was significantly greater than 34% in Liu et al. ($p<10^{-10}$,χ^2 test). Specifically, the 13 sequences (UniProt ID) we obtained were: ectodysplasin (Q92838), Na/K-transporting ATPase subunit γ (P54710), TNF receptor superfamily member 13B (O14836), Platelet glycoprotein IX (P14770), MPL (Thrombopoietin receptor) (P40238), MPZ (Myelin Protein P0) (P25189), caveolin-3 human (P56539), Neu/ErbB-2 receptor tyrosine-protein kinase rat (P06494), FGFR1 (P11362), TREM-2 Triggering receptor expressed on myeloid cells (Q9NZC2), FcγRIIb (Q8NI89), Mast/Stem cell growth factor receptor Kit (P10721) and GCSF receptor (Q99062).

Amino acid	Composition (count and (%)) in the disease-related TM helices of Moore et al. [3][1)]	Composition (%) in the TM helices database by Liu et al. [37]
L	84 (27.9)	16
V	41 (13.6)	8
A	34 (11.3)	9
I	32 (10.6)	10
G	27 (9.0)	8
F	18 (6.0)	8
C	16 (5.3)	2
T	12 (4.0)	7
S	11 (3.7)	7
Y	7 (2.3)	3
W	5 (1.7)	3
M	4 (1.3)	4
R	3 (1.0)	1
H	2 (0.7)	2
P	2 (0.7)	4
K	1 (0.3)	1
D	1 (0.3)	1
E	1 (0.3)	1
Q	0 (0)	2
N	0(0)	3
[1)] See the text for the specific entries of this set.		

Table 3: Amno acid composition of helical TM peptides.

Unlike G, A and S, which have small side chains, the branched chain amino acids V, L and I limit the access of peptide backbone to each other, also limiting electrostatic interactions (backbone-backbone interaction) with other molecules. So, the fact that a greater proportion is accounted for by V, L and I in the Moore et al.'s list [3] supports the importance of non-specific hydrophobic interactions for the dynamic interaction involved in the cell signaling mediated by disease-related TMs. We reason that polar side chains are underrepresented for such TM peptides because their electrostatic interactions tend to stabilize dimers, and not beneficial when dynamic interactions between TMs are necessary.

Overall, our results show that UA FFs show a significant level of inaccuracy the in dimerization propensity for the Leu- and Ala- rich TM helical peptides. As biomedically important helical peptides are rich in non-proline aliphatic amino acid residues (L, V, I and A), our data suggest that their lateral association tends to suffer considerable degrees of inaccuracy in the simulation analyses using the UA FFs. In our companion paper [22], we show that the parameter transferability of the UA FFs becomes deteriorates as the physiological realism of the TM peptides/membrane system increases.

References

1. Fleming KG (2014) Energetics of membrane protein folding. Annu Rev Biophys 43: 233-255.
2. Cymer F, Von Heijne G, White SH (2015) Mechanisms of integral membrane protein insertion and folding. J Mol Biol 427(5): 999-1022.
3. Moore DT, Berger BW, DeGrado WF (2008) Protein-protein interactions in the membrane: Sequence, structural, and biological motifs. Structure 16(7): 991-1001.
4. Endres NF, Das R, Smith AW, et al. (2013) Conformational Coupling across the plasma membrane in activation of the EGF Receptor. Cell 152(3): 543-556.
5. Bessman NJ, Bagchi A, Ferguson KM, et al. (2014) Complex relationship between ligand binding and dimerization in the epidermal growth factor receptor. Cell Rep 9(4): 1306-1317.
6. Fink A, Sal-Man N, Gerber D et al. (2012) Transmembrane domains interactions within the membrane milieu: Principles, advances and challenges. Biochim Biophys Acta 1818(4): 974-983.
7. Bocharov EV, Mineev KS, Pavlov KV, et al. (2017) Helix-helix interactions in membrane domains of bitopic proteins: Specificity and role of lipid environment. Biochim Biophys Acta 1859(4): 561-576.
8. Sarabipour S (2017) Parallels and distinctions in FGFR, VEGFR, and EGFR mechanisms of transmembrane signaling. Biochemistry 56(25): 3159-3173.
9. Castillo N, Monticelli L, Barnoud J (2013) Free energy of WALP23 dimer association in DMPC, DPPC, and DOPC bilayers. Chem Phys Lipids 169: 95-105.
10. Lelimousin M, Limongelli V, Sansom MS (2016) Conformational changes in the epidermal growth factor

receptor: Role of the transmembrane domain investigated by coarse-grained metadynamics free energy calculations. J Am Chem Soc 138(33): 10611-10622.

11. Hénin J, Pohorille A, Chipot C (2005) Insights into the Recognition and Association of Transmembrane α-Helices. The Free Energy of α-Helix Dimerization in Glycophorin A. J Am Chem Soc 127(23): 8478-8484.

12. Nishizawa M, Nishizawa K (2016) Free energy of helical transmembrane peptide dimerization in OPLS-AA/Berger force field simulations: inaccuracy and implications for partner-specific Lennard-Jones parameters between peptides and lipids. Molecular Simulation 42(11): 916-926.

13. Nishizawa M, Nishizawa K (2018) Sequence-nonspecific stabilization of transmembrane helical peptide dimer in lipid raft-like bilayers in atomistic simulations. I. Dimerization free energy and impact of lipid-peptide potential energy. Ann Biomed Res 1(1): 105.

14. Kaminski GA, Friesner RA, Tirado-Rives J et al (2001) Evaluation and reparametrization of the OPLS-AA force field for proteins via comparison with accurate quantum chemical calculations on peptides. J Phys Chem B 105(28): 6474-6487.

15. Berger O, Edholm O, Jähnig F (1997) Molecular dynamics simulations of a fluid bilayer of dipalmitoylphosphatidylcholine at full hydration, constant pressure, and constant temperature. Biophys J 72(5): 2002-2013.

16. Nishizawa M, Nishizawa K (2014) Potential of mean force analysis of the self-association of leucine-rich transmembrane α-helices: Difference between atomistic and coarse-grained simulations. J Chem Phys 141(7): 075101.

17. Yano Y, Kondo K, Kitani R et al. (2015) Cholesterol-induced lipophobic interaction between transmembrane helices using ensemble and single-molecule fluorescence resonance energy transfer. Biochemistry 54(6): 1371-1379.

18. Tieleman DP, MacCallum JL, Ash WL, et al. (2006) Membrane protein simulations with a united-atom lipid and all-atom protein model: lipid–protein interactions, side chain transfer free energies and model proteins. J Phys Condens Matter 18(28): S1221 -1234.

19. de Jong DH, Periole X, Marrink SJ (2012) Dimerization of amino acid side chains: lessons from the comparison of different force fields. J Chem Theory Comput 8(3): 1003-1014.

20. Mirjalili V, Feig M (2015) Interactions of amino acid side-chain analogs within membrane environments. J Phys Chem B 119(7): 2877-2885.

21. Mall S, Broadbridge R, Sharma RP, et al. (2001) Self-association of model transmembrane α-helices is modulated by lipid structure. Biochemistry 40(41): 12379-12386.

22. Nishizawa K, Nishizawa M (2018) Force-field dependency of Leu-rich helical peptides dimerization energy in lipid bilayers. II. Limited transferability of united-atom simulation parameters to membrane-water interfaces. Ann Biomed Res 1(2): 113.

23. Nishizawa K, Nishizawa M, Gnanasambandam R, et al. (2015) Effects of Lys to Glu mutations in GsMTx4 on membrane binding, peptide orientation, and self-association propensity, as analyzed by molecular dynamics simulations. Biochim Biophys Acta 1848(11): 2767-2778.

24. Poger D, Mark AE (2010) On the validation of molecular dynamics simulations of saturated and cis-monounsaturated phosphatidylcholine lipid bilayers: A Comparison with experiment. J Chem Theory Comput 6(1): 325-336.

25. Domański J, Stansfeld P, Sansom MSP, et al. (2010) Lipidbook: A public repository for force field parameters used in membrane simulations. J Membrane Biol 236(3): 255-258.

26. Oostenbrink C, Villa A, Mark AE, et al. (2004) A biomolecular force field based on the free enthalpy of hydration and solvation: the GROMOS force-field parameter sets 53A5 and 53A6. J Comput Chem 25(13): 1656-1676.

27. Chiu SW, Clark MM, Jakobsson E, et al. (1999) Optimization of hydrocarbon chain interaction parameters: Application to the simulation of fluid phase lipid bilayers. The J Phys Chem B 103(30):6323-6327.

28. Chiu SW, Pandit SA, Scott HL, et al. (2009) An improved united atom force field for simulation of mixed lipid bilayers. J Phys Chem B 113(9): 2748-2763.

29. Huang J, MacKerell Jr AD (2013) CHARMM36 all-atom additive protein force field: Validation based on comparison to NMR data. J Comput Chem 34(25): 2135-2145.

30. Klauda JB, Venable RM, Freites JA, et al. (2010) Update of the CHARMM all-atom additive force field for lipids: Validation on six lipid types. J Phys Chem B 114(23): 7830-7843.

31. Lee S, Tran A, Allsopp M (2014) CHARMM36 united atom chain model for lipids and surfactants. J Phys Chem B 118(2): 547-556.

32. Jorgensen WL, Madura JD, Swenson CJ (1984) Optimized intermolecular potential functions for liquid hydrocarbons. J Am Chem Soc 106(22): 6638-6646.

33. Hess B, Bekker H, Berendsen HJC, et al. (1997) LINCS: A linear constraint solver for molecular simulations. J Comput Chem 18: 1463-1472.

34. Miyamoto S, Kollman PA (1992) SETTLE: An analytical version of the SHAKE and RATTLE algorithm for rigid water models. J Comput Chem 13: 952-962.

35. Darden T, York D, Pedersen L (1993) Particle mesh Ewald: An N· log (N) method for Ewald sums in large systems. J Chem Phys 98(12): 10089-10092.

36. Kumar S, Rosenberg JM, Bouzida D (1992) The weighted histogram analysis method for free-energy calculations on biomolecules. I. The method. J Comp Chem 13: 1011-1021.

37. Liu Y, Engelman DM, Gerstein M (2002) Genomic analysis of membrane protein families: abundance and conserved motifs. Genome Biol 3(10): research 0054-1.

Nishizawa M, Nishizawa K (2018) Force-field Dependency of Leu-rich Helical Peptides Dimerization Energy in Lipid Bilayers. I. United-atom Simulations Show Discrepancy from Experiments and All-atom Simulations. Ann Biomed Res 1: 112.

***Corresponding author:** Kazuhisa Nishizawa, MD, PhD, Department of Clinical Laboratory Science, Teikyo University School of Medical Technology, 2 Kaga, Itabashi, Tokyo, 173-8605 Japan, Tel: +81-3-3964-1211; Email: kazunet@med.teikyo-u.ac.jp

Received date: October 06, 2018; **Accepted date:** October 10, 2018; **Published date:** October 12, 2018

Citation: Nishizawa M, Nishizawa K (2018) Force-field Dependency of Leu-rich Helical Peptides Dimerization Energy in Lipid Bilayers. I. United-atom Simulations Show Discrepancy from Experiments and All-atom Simulations. *Ann Biomed Res* 1(2): 112.

Copyright: Nishizawa M, Nishizawa K (2018) Force-field Dependency of Leu-rich Helical Peptides Dimerization Energy in Lipid Bilayers. I. United-atom Simulations Show Discrepancy from Experiments and All-atom Simulations. Ann Biomed Res 1(2): 112.

Berger phospholipids [15]					
		name	σ	ε	
DOPC		LC3	3.960120e-01	6.064938e-01	CH_3 of choline
		LNL	3.249967e-01	7.113774e-01	N of choline
		LH2	3.905043e-01	4.936368e-01	CH_2 bonded to choline N
		LC2	3.799786e-01	4.939498e-01	C of glycerol forming −C−O−P−
		LP	3.740042e-01	8.367132e-01	P of phosphate
		LOS	2.999886e-01	8.791447e-01	O of −C−O−P− and −C−O−C−
		LOM	2.959999e-01	8.786943e-01	O of P=O
		LH1	3.800152e-01	3.346162e-01	C of −CH=CH− of unsaturated acyl chain; C of glycerol backbone bonded to phosphate
		LC	3.749857e-01	4.395244e-01	C of carbonyl
		LO	2.959999e-01	8.786943e-01	O of carbonyl
		LP2	3.959944e-01	3.808375e-01	acyl chain methylene CH_2
		LP3	3.960063e-01	5.689493e-01	acyl chain terminal CH_3
OPLS-AA (all atom) [14]					
Ala, Leu,Lys	name	bond_type	σ	ε	
	opls_237	N	3.25000e-01	7.11280e-01	N for NH_2 capping C-terminal
	opls_240	H	0.00000e+00	0.00000e+00	H for NH_2 capping C-terminal
	opls_140	HC	2.50000e-01	1.25520e-01	H bonded to Cα
	opls_238	N	3.25000e-01	7.11280e-01	N for backbone
	opls_241	H	0.00000e+00	0.00000e+00	H for backbone N-H
	opls_224B	CT_2	3.50000e-01	2.76144e-01	Cα for backbone
	opls_235	C	3.75000e-01	4.39320e-01	C for backbone
	opls_236	O	2.96000e-01	8.78640e-01	O for backbone
	opls_267	C	3.75000e-01	4.39320e-01	C for C-terminal COOH
	opls_268	OH	3.00000e-01	7.11280e-01	O for C-terminal COOH
	opls_269	O_3	2.96000e-01	8.78640e-01	OT for C-terminal COOH
	opls_270	HO	0.00000e+00	0.00000e+00	HO for C-terminal COOH
	opls_135	CT	3.50000e-01	2.76144e-01	Cβ of ALA or Cδ1,Cδ2 of LEU
	opls_136	CT	3.50000e-01	2.76144e-01	CB of LEU
	opls_137	CT	3.50000e-01	2.76144e-01	CG of LEU
	opls_292	CT	3.50000e-01	2.76144e-01	CE of Lys
	opls_287	NZ	3.25000e-01	7.11280e-01	NZ of Lys
	opls_290	H3	0.00000e+00	0.00000e+00	H of Lys side chain NH_3
GROMOS 53a6 [24,26]					
DOPC		CH3L	3.747918e-01	8.671503e-01	CH_3 of choline
		NL	3.136473e-01	6.397949e-01	N of choline
		CH2	4.070381e-01	4.105424e-01	CH_2 of acyl chain; CH_2 of choline
		OA	2.954842e-01	8.496074e-01	O of −C−O−P−
		P	3.385567e-01	2.446744e+00	P of phosphate
		OML	2.625854e-01	1.725044e+00	O of P=O
		CH1	5.019182e-01	9.488933e-02	C of glycerol backbone bonded to phosphate
		OE	2.849161e-01	1.057114e+00	O of −C−O−C−
		C	3.581179e-01	2.774057e-01	C of carbonyl
		O	2.760065e-01	1.279109e+00	O of carbonyl
		CR1	3.741191e-01	5.026588e-01	C of −CH=CH− of unsaturated acyl chain

	CH3	3.747918e-01	8.671503e-01	CH_3 of acyl chain terminus
Ala, Leu,Lys,Ile and Val	NL	3.136473e-01	6.397949e-01	N of NH3 of Lys sidechain
	N	3.136473e-01	6.397949e-01	N of backbone amide
	H	0	0	H of backbone amide, H of NH3 of Lys sidechain
	CH1	5.019182e-01	9.488933e-02	Cα for non-Gly amino-acids, Leu Cγ, Ile Cβ, Val Cβ,
	CH2	4.070381e-01	4.105424e-01	Leu Cβ, Ile Cγ1, Lys Cβ,Cγ, Cδ, Cε
	CH3	3.747918e-01	8.671503e-01	Ala Cβ, Leu Cγ1, Cγ2, Ile Cγ2, Cδ; Val Cγ1, Cγ2
	C	3.581179e-01	2.774057e-01	C of backbone carbonyl
	O	2.760065e-01	1.279109e+00	O of backbone carbonyl
	NT	3.572200 e-01	2.931403e-01	N of NH_2 capping C-terminus
Charmm36 [29,30]				
DOPC	NTL	0.329632525712	0.8368	N of choline
	CTL5	0.367050271874	0.33472	C of choline CH_3
	CTL2	0.358141284692	0.23430	methylene carbon of choline, C of CH_2 of acyl chain
	HL	0.12472582054	0.19246	H of choline CH_3, H of methylene of choline
	HAL2	0.238760856462	0.11715	H of choline CH_2, H of CH_2 of acylchain
	PL	0.3830864488	2.44764	P of phosphate
	O2L	0.302905564168	0.50208	O of P=O
	OSLP	0.293996576986	0.4184	O of −O−P−O−
	CTL1	0.405358916754	0.08368	C of glycerol backbone bonded to phosphate
	HAL1	0.235197261589	0.09205	H bonded to glycerol backbone C bonded to phosphate
	OSL	0.293996576986	0.4184	ester O linking glycerol backbone to fatty acid
	CL	0.356359487256	0.29288	C of carbonyl
	OBL	0.302905564168	0.50208	O of carbonyl
	CEL1	0.372395664183	0.28451	CH of −CH=CH− of unsaturated acyl chain
	HEL1	0.222724679535	0.12970	H of −CH=CH− of unsaturated acyl chain
	CTL3	0.363486677001	0.32635	C of acyl chain terminus
	HAL3	0.238760856462	0.10042	H of acyl chain terminus CH_3
Ala, Leu, Ile, Val and Lys	NH2	0.329632525712	0.8368	N of NH_2 capping C-terminus
	NH1	0.329632525712	0.8368	N of backbone amide
	H	0.040001352445	0.19246	H of backbone amide
	CT1	0.356359487256	0.13389	Cα for non-Gly amino acids; Leu Cγ; Ile Cβ; Val Cβ;
	CT2	0.358141284692	0.23430	Leu Cβ, Ile Cγ1, Lys Cβ,Cγ, Cδ, Cε
	CT3	0.363486677001	0.32635	Leu Cδ1, Cδ2; Ala Cβ; Ile Cγ2, Cδ; Val Cγ1, Cγ2
	HB1	0.235197261589	0.09205	H bonded to Cα for non-Gly amino acids
	HA1	0.238760856462	0.18828	H bonded to CT1 except Cα
	HA2	0.238760856462	0.14226	H bonded to CT2 except Cα
	HA3	0.238760856462	0.10042	H bonded to CT3 except Cα
	C	0.356359487256	0.46024	C of backbone carbonyl
	O	0.302905564168	0.50208	O of backbone carbonyl
	NH3	0.329632525712	0.8368	N of NH_3 of Lys sidechain
	HC	0.040001352445	0.19246	H of NH_3 of Lys sidechain
Charmm-UA [31]				
DOPC (the parameters not listed here are the same as Charmm36)	CH1E	0.38005739316	0.48116	CH of −CH=CH− of unsaturated acyl chain
	CH2E	0.39056999803	0.493712	CH_2 of acyl chain
	CH3E	0.39056999803	0.73220	CH_3 of acyl chain terminus

[1)] Only the amino acid and lipid species relevant to this study are presented.

Appendix Table A1 : LJ parameters of DOPC, Leu and Ala used in the FFs used in the present study[1)].